*Bioinformatics*, 36(9), 2020, 2796–2804
doi: 10.1093/bioinformatics/btaa066
Advance Access Publication Date: 31 January 2020
Original Paper

Gene expression

# Statistical inference of differential RNA-editing sites from RNA-sequencing data by hierarchical modeling

**Stephen S. Tran[1], Qing Zhou[1,2,*] and Xinshu Xiao[1,3,4,5,*]**

[1]Bioinformatics Interdepartmental Program, [2]Department of Statistics, [3]Department of Integrative Biology and Physiology, [4]Molecular Biology Institute and [5]Institute for Quantitative and Computational Biology, UCLA, Los Angeles, CA 90095, USA

*To whom correspondence should be addressed.
Associate Editor: Jan Gorodkin

Received on July 25, 2019; revised on December 29, 2019; editorial decision on January 22, 2020; accepted on January 24, 2020

## Abstract

**Motivation:** RNA-sequencing (RNA-seq) enables global identification of RNA-editing sites in biological systems and disease. A salient step in many studies is to identify editing sites that statistically associate with treatment (e.g. case versus control) or covary with biological factors, such as age. However, RNA-seq has technical features that incumbent tests (e.g. *t*-test and linear regression) do not consider, which can lead to false positives and false negatives.

**Results:** In this study, we demonstrate the limitations of currently used tests and introduce the method, RNA-editing tests (REDITs), a suite of tests that employ beta-binomial models to identify differential RNA editing. The tests in REDITs have higher sensitivity than other tests, while also maintaining the type I error (false positive) rate at the nominal level. Applied to the GTEx dataset, we unveil RNA-editing changes associated with age and gender, and differential recoding profiles between brain regions.

**Availability and implementation:** REDITs are implemented as functions in R and freely available for download at https://github.com/gxiaolab/REDITs. The repository also provides a code example for leveraging parallelization using multiple cores.

**Contact:** zhou@stat.ucla.edu or gxxiao@ucla.edu

**Supplementary information:** Supplementary data are available at *Bioinformatics* online.

## 1 Introduction

RNA editing alters RNA sequences by base modifications, insertions and deletions, which in metazoans (Yablonovitch *et al.*, 2017), predominantly consists of adenosine to inosine (A-to-I) changes catalyzed by the adenosine deaminase acting on RNA (ADAR) proteins. A plethora of studies have demonstrated diverse biological roles for A-to-I editing. The most-studied type of RNA editing consists of recoding sites. Because inosines are recognized as guanosines by the cellular machinery, such editing sites can lead to amino acid substitutions in proteins. Functional studies have implicated many of these protein-recoding sites in modulating neuronal function, synaptic permeability and emissions (Behm and Öhman, 2016). In contrast, RNA editing in non-coding regions is less well-understood, despite the vast number of sites. Nonetheless, the functional relevance of such editing sites is starting to be elucidated, such as in splicing regulation (Feng *et al.*, 2006; Hsiao *et al.*, 2018; Rueter *et al.*, 1999), microRNA targeting and polyadenylation of 3′ UTRs (Bahn *et al.*, 2015; Brummer *et al.*, 2017; Nishikura, 2016) and modulation of double-stranded RNA-related immunity (Liddicoat *et al.*, 2015). Importantly, widespread aberrant RNA-editing patterns have been reported across a large number of diseases, including neurological diseases (Hideyama *et al.*, 2012; Tran *et al.*, 2019), atherosclerosis (Stellos *et al.*, 2016), cancer (Fumagalli *et al.*, 2015; Han *et al.*, 2015; Ishizuka *et al.*, 2019; Paz-Yaacov *et al.*, 2015) and autoimmune disorders (Roth *et al.*, 2018).

Recent studies of RNA editing were greatly facilitated by the RNA-sequencing (RNA-seq) technology and related bioinformatic tools, which allow comprehensive delineation of global editomes in diverse biological processes. In editome profiling, a critical task is to identify editing sites that are statistically different in their quantitative levels between two groups of samples (such as disease versus controls). Alternatively, editing sites whose levels are statistically associated with certain variables, such as age, are sought after. Most previous studies utilized the classic *t*-test (Hwang *et al.*, 2016; Kang *et al.*, 2015; Qin *et al.*, 2014), Wilcoxon rank-sum test (Han *et al.*, 2015; Kang *et al.*, 2015; Roth *et al.*, 2018; Srivastava *et al.*, 2017; Tran *et al.*, 2019), Fisher's exact test (Paz *et al.*, 2007; Quinones-Valdez *et al.*, 2019; Tan *et al.*, 2017; Tran *et al.*, 2019) or linear regression-based test (Brummer *et al.*, 2017; Chen *et al.*, 2013; Hwang *et al.*, 2016; Picardi *et al.*, 2015; Tan *et al.*, 2017; Tran *et al.*, 2019) for these purposes. However, these tests are limited due to the lack of consideration of uncertainty in the read counts or variability in editing quantification between biological replicates.

Here, we develop and evaluate a suite of tools, RNA-editing tests (REDITs), that are built upon beta-binomial-based models to carry out differential editing analyses. Specifically, REDITs consist of two methods. The first method handles the classic case of identifying editing sites that possess differential editing levels between two conditions (i.e. case versus control). The second method carries out statistical inference of categorical or quantitative variables that covary with editing levels (e.g. age-correlated RNA editing). Beta-binomial models have been applied to analyze DNA methylation (Dolzhenko and Smith, 2014; Feng *et al.*, 2014; Hebestreit *et al.*, 2013; Park *et al.*, 2014; Sun *et al.*, 2014). However, these methods are not directly applicable to RNA-editing studies due to their methylation-specific aspects (e.g. methylome-wide priors).

We show via simulated and actual data that REDITs have improved sensitivity and mitigated false-positive rate compared to commonly used alternatives. Applied to human tissue editomes (GTEx), REDITs revealed novel insights on the association of RNA editing with age, gender and differential recoding profiles between brain regions.

## 2 Materials and methods

### 2.1 Beta-binomial model underlying REDITs

We first consider an A-to-G editing site measured using RNA-seq across $m$ samples from two conditions (Fig. 1a). For each sample $m_i$, we denote the total read coverage as $n_i$ and the number of reads harboring the edited nucleotide as $k_i$. As in most previous studies, the observed editing level can be calculated as $k_i/n_i$. If we assume the true underlying editing level is $\theta_i$, then $k_i$ follows a binomial distribution:

$$k_i|\theta_i \sim \text{Binomial}(n_i,\ \theta_i),$$
$$P(k_i|\theta_i) = \binom{n_i}{k_i}\theta_i^{k_i}(1-\theta_i)^{n_i-k_i}.$$

The value of $\theta_i$ is expected to vary amongst samples due to biological variability. Thus, we model $\theta_i$ using a beta distribution for samples from the same condition. More specifically, for condition 1:

$$\theta_i \sim Beta(\alpha_1,\beta_1)$$
$$P(\theta_i) = \frac{\theta_i^{\alpha_1-1}\cdot(1-\theta_i)^{\beta_1-1}}{B(\alpha_1,\beta_1)}, i = 1\ldots j.$$

For condition 2:

$$\theta_i \sim Beta(\alpha_2,\beta_2)$$
$$P(\theta_i) = \frac{\theta_i^{\alpha_2-1}\cdot(1-\theta_i)^{\beta_2-1}}{B(\alpha_2,\beta_2)}, i = j+1\ldots m,$$

where $\alpha,\beta$ are hyper parameters and $B(\alpha,\beta)$ is the beta function. We choose the beta distribution because it adheres to the restriction that editing levels must fall in a continuum between (0, 1). Additionally, the beta distribution is conjugate to the binomial distribution (below), which eases our inference procedure. Given the inordinate flexibility of both concave and convex shapes possessed by the beta distribution, we restricted $\alpha \geq 1$ and $\beta \geq 1$ to enforce that it partake only uniform or unimodal shapes and eschew U-shapes. Intuitively, this restriction presumes that the distribution of true-editing levels per condition has measures of centrality and dispersion that approximately correspond to the peak and width of the distribution, respectively. In addition, these parameter restrictions were observed for all editing sites analyzed in the GTEx dataset (Section 3) (Supplementary Fig. S1a). In totality, each sample follows a generative model whereby its true editing level $\theta_i$ is an observation from a uniform or unimodal beta distribution characteristic of its condition, and the random consampling of edited reads or non-edited reads from RNA-seq follows a binomial distribution (Fig. 1b). The entire generative model is a beta-binomial distribution:

$$P(k_i,\theta_i|n_i,\alpha_l,\beta_l) = P(k_i|\theta_i,n_i)\cdot P(\theta_i|\alpha_l,\beta_l),$$
$$= \binom{n_i}{k_i}\theta_i^{k_i}(1-\theta_i)^{n_i-k_i}\cdot\frac{\theta_i^{\alpha_l-1}(1-\theta_i)^{\beta_l-1}}{B(\alpha_l,\beta_l)},$$

where $l = 1$ for $i \leq j$ and $l = 2$ for $i \geq j+1$.

Integrating over $\theta_i$ yields the marginal likelihood of $k_i$ given the hyper-parameter $(\alpha,\ \beta)$ :

$$P(k_i|n_i,\ \alpha_l,\ \beta_l) = \int_0^1 \binom{n_i}{k_i}\theta_i^{k_i}(1-\theta_i)^{n_i-k_i}\cdot\frac{\theta_i^{\alpha_l-1}\ (1-\theta_i)^{\beta_l-1}}{B(\alpha_l,\beta_l)}d\theta_i$$
$$= \binom{n_i}{k_i}/B(\alpha_l,\beta_l)\int_0^1\theta_i^{k_i}(1-\theta_i)^{n_i-k_i}\cdot\theta_i^{\alpha_l-1}\ (1-\theta_i)^{\beta_l-1}\ d\theta_i$$
$$= \binom{n_i}{k_i}/B(\alpha_l,\beta_l)\int_0^1\theta_i^{k_i+\alpha_l-1}\ (1-\theta_i)^{n_i-k_i+\beta_l-1}\ d\theta_i$$
$$= \binom{n_i}{k_i}\cdot\frac{B(k_i+\alpha_l,n_i-k_i+\beta_l)}{B(\alpha_l,\beta_l)}\ . \tag{1}$$

### 2.2 Statistical inference of differential editing between two groups

Given two groups of samples (e.g. cases and controls), under the null hypothesis of no between-group difference on editing (i.e. $\alpha_1 = \alpha_2 = \alpha_0$ and $\beta_1 = \beta_2 = \beta_0$), the likelihood of the data is given by:

$$L_0 = \prod_1^m P(k_i|n_i,\ \alpha_0,\ \beta_0) = \prod_1^m\binom{n_i}{k_i}\cdot\frac{B(k_i+\alpha_0,n_i-k_i+\beta_0)}{B(\alpha_0,\beta_0)}\ .$$

The likelihood of the alternative model where significant difference exists between the two groups is given by:

$$L_A = \prod_{i=1}^j P(k_i|n_i,\ \alpha_1,\ \beta_1)\prod_{i=j+1}^m P(k_i|n_i,\ \alpha_2,\ \beta_2)$$
$$= \prod_{i=1}^j\binom{n_i}{k_i}\cdot\frac{B(k_i+\alpha_1,n_i-k_i+\beta_1)}{B(\alpha_1,\beta_1)}$$
$$\cdot\prod_{i=j+1}^m\binom{n_i}{k_i}\cdot\frac{B(k_i+\alpha_2,n_i-k_i+\beta_2)}{B(\alpha_2,\beta_2)}.$$

Wilk's theorem states that the statistical significance of differential editing is given by:

$$-2\cdot\log\left(\frac{L_0}{L_A}\right)\sim\chi^2,\ \text{with two degrees of freedom,}$$

where $L_0$ and $L_A$ are evaluated at the maximum likelihood estimates (MLEs) of $\alpha$'s and $\beta$'s. Thus, we call this method REDIT-LLR henceforth.

### 2.3 Statistical inference of editing sites that covary with quantitative variables

The beta-binomial model can be expanded to handle statistical inference under the regression scenarios (REDIT-Regression). For

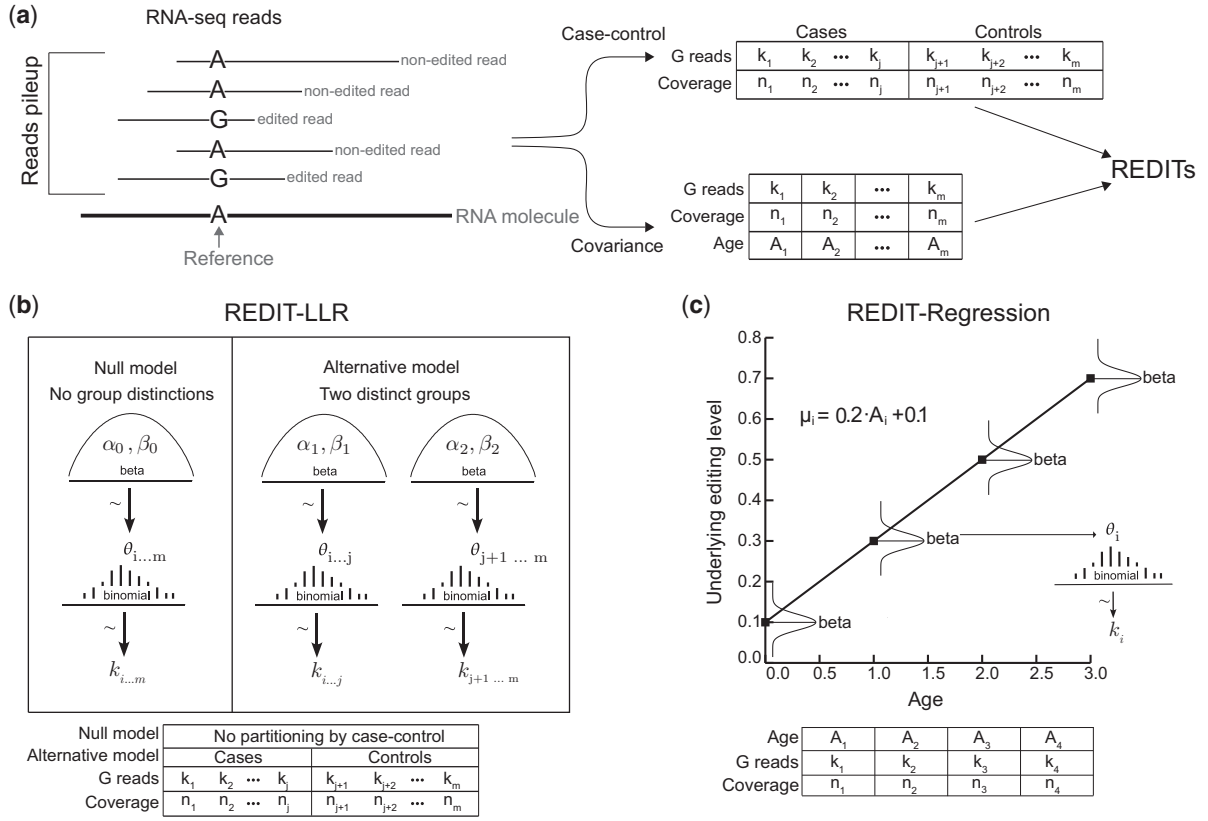


**Fig. 1.** Overview of REDITs. (**a**) Context for usage of REDITs within RNA-editing studies. RNA-seq is generated on multiple samples ($i = 1 \ldots m$), and editing sites are quantified by counting number of matches/non-edited reads (A-containing) and mismatches/edited reads (G-containing). $k_i$ =# of G-containing reads and total coverage $n_i$ =# of A reads+# of G reads. Depending on the type of inference sought, samples are partitioned into tables, which are input into REDITs for statistical inference. (**b**) Overview of REDIT-LLR for case–control inference. Under the null model, a single beta distribution characterizes the underlying editing levels $\theta_{1\ldots m}$ of all samples, whereas the alternative model posits distinct beta distributions characterizing condition 1 ($\theta_{1\ldots j}$) against condition 2 ($\theta_{j+1\ldots m}$). A binomial distribution characterizes edited reads per sample ($k_{1\ldots m}$). The coverage acquired via RNA-seq directly determines $n_{1\ldots m}$. (**c**) Overview of REDIT-Regression for inference of covariance with RNA editing. For simplicity, the model is depicted showing covariance of editing with age in four samples. The underlying editing level of each sample is characterized by a distinct beta distribution where mean ($u_i$) is linearly dependent on age through $u_i$=0.2 $A_i$ +0.1, and dispersion ($\sigma$) is constant. Points along regression line show locations of the means ($u_i$) of beta distributions. The number of edited reads ($k_i$) then follow a binomial ($k_i|n_i, \theta_i$) distribution where $n_i$ is determined by sequencing coverage per sample at this editing site, and $\theta_i$ is an observation from the respective beta distribution per sample

convenience, we describe this method using the example of identification of editing sites that covary with age ($A_i$). For a specific editing site, we assume the underlying true-editing levels per sample, ($\frac{k_i}{n_i} \sim \theta_i$) ($i = 1 \ldots m$), follow a beta distribution with constant dispersion ($\sigma$) but with mean ($\mu$) linearly dependent on age (Fig. 1c). The assumption of a constant $\sigma$ and the dependency of $\mu$ on age are analogous to that of linear regression. We re-parameterize the beta-binomial model as follows,

$$\mu = \frac{\alpha}{\alpha + \beta}$$

$$\sigma = \frac{1}{\alpha + \beta}.$$

Then, the marginal likelihood of $k_i$ in Equation (1) becomes:

$$P(k_i|n_i,\ u_i,\ \sigma) = \binom{n_i}{k_i} \frac{B\left(k_i + \frac{\mu_i}{\sigma}, n_i - k_i + \frac{1-\mu_i}{\sigma}\right)}{B\left(\frac{\mu_i}{\sigma}, \frac{(1-\mu_i)}{\sigma}\right)}.$$

The dependency of $\mu$ on age is linear:

$$\mu_i = \beta_{age} \cdot A_i + \beta_0.$$

Under the above re-parameterization, $\mu$ must fall between (0, 1) and $\sigma$ must be $> 0$, which we enforce during MLE. The likelihood of the data is given by:

$$L_{\text{data}} = \prod_{i=1}^{m} P(k_i|n_i,\ \mu_i,\ \sigma) = \prod_{i=1}^{m} \binom{n_i}{k_i} \frac{B\left(\frac{k_i+\mu_i}{\sigma}, n_i - k_i + \frac{1-\mu_i}{\sigma}\right)}{B\left(\frac{\mu_i}{\sigma}, \frac{(1-\mu_i)}{\sigma}\right)}.$$

The null hypothesis $H_0$ is that age does not impact editing, i.e. $\beta_{\text{age}} = 0$ or equivalently $\mu_i = \beta_0$. Based on Wilk's theorem, the statistical significance of the alternative model ($H_A$: $\beta_{\text{age}} \neq 0$) is given by:

$$-2 \cdot \log\left(\frac{L_0}{L_A}\right) \sim \chi^2, \text{with one degree of freedom,}$$

where $L_0$ and $L_A$ are maximum likelihood under $H_0$ and $H_A$, respectively. General inference of multiple covariates ($\beta_1, \beta_2, \ldots$) with respective observations ($X_{1i}, X_{2i}, \ldots$) can be carried out by comparing maximum likelihood under the alternative model, $\mu_i = \beta_1 \cdot X_{1i} + \beta_2 \cdot X_{2i} + \cdots + \beta_0$, to maximum likelihood under null models with $\beta_j = 0$ to determine statistical association of covariate $j$ with editing for each $j = 1,2,\ldots$. Categorical variables (e.g. gender and ethnicity) can also be included by encoding them as 0 and 1. Regression for one or more quantitative and/or categorical covariates is handled by our provided code (see code availability).

For regressions of proportions (values restricted between 0 and 1), the $\mu$ term is conventionally transformed using a logistic link function:

$$\mu_i = \frac{1}{1 + e^{-(\beta_{age} \cdot A_i + \beta_0)}}.$$

However, the logistic transformation can over-fit the data and lead to inflated maximum likelihood ratios. Thus, we chose not to use the logistic link function and instead opted to constrict regression coefficients within the MLE so that editing levels would never fall below 0 or above 1.

### 2.4 Simulations to evaluate REDIT-LLR

To simulate RNA-editing data, we extracted RNA-editing sites from the REDIportal database (Picardi *et al.*, 2017) derived from 2660 GTEx samples and other sources. Using these data, we simulated realistic read coverages and hyper-parameter distributions reflecting biological variance of editing levels. First, we used MLE to fit beta distributions to the editing levels of each editing site in brain samples of GTEx. Brain was chosen since it has the largest sample size among all histological types (Supplementary Table S1a). Furthermore, to acquire highly accurate parameters, we required the editing sites to have ≥20 reads in ≥250 brain samples. A total of 1206 editing sites were retained. The $\alpha$ and $\beta$ parameters were then clustered ($k$-means) into 10 clusters, yielding 10 representative parameter values (Supplementary Fig. S1a and b and Table S1b). As an alternative, we repeated the simulations using a truncated Gaussian distribution instead of beta distribution. The mean and variance parameters were converted directly from the mean and variance of the beta distributions (Supplementary Fig. S1d and Table S1b).

Editing levels were sampled from the beta or truncated Gaussian distributions, and the numbers of edited reads for each sample were simulated using the corresponding binomial distribution. To simulate read coverages, we used MLE to fit negative binomial distributions to the coverage data of the above editing sites from 10 random GTEx brain samples (Supplementary Table S1c and Fig. S1c). A total of 100 independent simulations of 1000 editing sites were created for each group, with 2, 3 or 5 samples per group.

### 2.5 Evaluating sensitivity and false-positive rates of REDIT-LLR

The false-positive rate and sensitivity of REDIT-LLR were evaluated by simulating case–control scenarios where the case and control groups were each characterized by 1 of the 10 beta (or truncated Gaussian) distributions (Supplementary Fig. S1). Sensitivity was evaluated where the cases and controls were simulated using different underlying distributions, and false-positive rate was evaluated using identical distributions to generate cases and controls. A $P < 0.05$ was imposed to call significant comparisons. We piloted evaluation of sensitivity and false-positive rate on a single set of parameters for a case–control comparison of three replicates, where the parameters for sensitivity were beta($\alpha = 13.52$, $\beta = 11.95$) versus beta($\alpha = 43.64$, $\beta = 0.23$), and parameters for false positives were beta($\alpha = 13.52$, $\beta = 11.95$) for both groups; simulations were then expanded to include all combinations of parameters and sample sizes.

Pooled Fisher's exact test, $t$-tests and Wilcoxon rank-sum tests were also applied on the above simulated editing sites. Pooled Fisher's exact test was carried out by pooling reads from replicates and testing the resulting 2×2 contingency table. The $t$-test and Wilcoxon rank-sum tests were performed in two ways, respectively, (i) using editing levels estimated without minimal read coverage requirement, and (ii) filtering out, for each editing site, any sample with read coverage <10 (i.e. thresholded $t$-test or Wilcoxon rank-sum test).

### 2.6 Evaluating false-positive rates of REDIT-Regression using simulated data

To evaluate REDIT-Regression, we simulated editing sites that covary with age. We based the simulations on a previous dataset of 33 postmortem human brains spanning fetal stages to old age (Hwang *et al.*, 2016). A total of 267 766 editing sites were reported by this study.

To test the false-positive rates, we simulated editing sites where age had no effect on editing level. For each editing site, we extracted its read coverage in each sample of the original dataset. The editing level and number of edited reads were simulated similarly as described for REDIT-LLR, using the beta or truncated Gaussian distributions (Supplementary Fig. S1). For each editing site, 1 of the 10 beta or truncated Gaussian distributions, respectively, was randomly selected to simulate edited reads. Each simulation included 3, 5, 7 and 33 samples and 267 766 editing sites, with the age values of the samples unaltered. For sample, sizes of 3, 5 and 7 we chose to use samples (R5805, R3523, R3990), (R5805, R3591, R3497, R4371, R3990) and (R5805, R5815, R3552, R3497, R4054, R3539, R3990), respectively, as these samples represented the age range of the dataset. Each simulation included editing sites where median coverage was at least 5 (93 437 sites for $n = 3$ 86 290 for $n = 5$ 68 235 for $n = 7$ and 90 919 for $n = 33$), and 100 independent simulations were carried out per sample size. For each simulation, the false-positive rate was calculated as the fraction of sites with significant age associations (REDIT-Regression $P < 0.05$) among all sites tested. We piloted the simulations on the sample size of three and then expanded to the other sample sizes.

Binomial regression, LIMMA, linear regression and thresholded linear regression (using samples with read coverage ≥10) were also performed for the above simulated data.

### 2.7 Evaluating sensitivity of REDIT-Regression using simulated data

To test sensitivity, we simulated various correlations between age and editing levels. First, we estimated representative correlations of these two variables using the original data of the 33 postmortem samples. We used editing sites where ≥20 samples had ≥20 read coverage. The observed editing levels (calculated as the number of edited reads divided by read coverage) were then regressed against age using linear regression. To tractably limit the number of simulated age-associations, we used a stricter $P$-value threshold of $P < 0.005$ to deem editing sites significant. These sites were used to derive five representative slope and intercept values to simulate linear relationships between age and editing levels (Supplementary Table S1d).

Using the above relationships, we simulated true-editing levels of each editing site by randomly sampling from a beta or truncated Gaussian distribution whose mean was set as $\mu_i = \beta_{age} \cdot A_i + \beta_0$, where $A_i$ was the unaltered age of the sample. The SD for each editing site was randomly selected from the standard deviations of the 10 distributions from the GTEx data described above. Other aspects of the simulations are similar as described for false-positive evaluation. Sensitivity was calculated as the fraction of editing sites with significant ($P < 0.05$) age association among all sites tested. We piloted sensitivity evaluation on sample size of three and where true-editing level was a beta distribution with mean set as $\mu_i = 0.005 \cdot A_i + 0.33$ and then expanded to the other four slopes and intercept values and sample sizes.

### 2.8 Evaluating false-positive rates and sensitivity of REDITs on actual data

To test the false-positive rate of REDIT-LLR on real data, we obtained 6814 editing sites in 18 control samples from a previous study of system lupus erythematosus (Hung *et al.*, 2015; Quinones-Valdez *et al.*, 2019). We randomly permuted the samples and formed two groups ($n = 2$, 3, 5, 10, 15 or 18 per group). Thus, any editing site called with $P < 0.05$ is deemed a false positive.

To test the sensitivity of REDIT-LLR on actual data, we obtained 12 258 editing sites from a previous study comparing two replicates of ADAR1 knock-down (KD) and controls in U87 cells (Bahn *et al.*, 2012). We reasoned that most editing sites should have reduced editing levels following ADAR1 KD. Thus, the total number

of differential editing sites ($P < 0.05$) called by each method was used as a proxy for sensitivity.

For REDIT-Regression, we used 267 766 editing sites from the 33 postmortem brains (Hwang *et al.*, 2016) as described above and randomly grouped samples with replacement to achieve various sample sizes ($n = 5, 10, 15, 20, 25, 30, 33$). Each sample was then randomly assigned a covariate value (1–$n$). Each random sampling and covariate assignment was repeated 100 times.

### 2.9 Application of REDIT-Regression to identify age- and gender-associated RNA editing

We applied REDIT-Regression to the GTEx dataset to investigate how RNA editing varies with human age and gender (4 668 508 editing sites obtained from the REDIportal database). To expedite run-time, we removed GTEx tissues that had fewer than 10 samples, and required editing sites to have ≥1 read coverage in ≥10 samples. We also adjusted for latent confounding factors by performing imputation and surrogate variable analysis (SVA) with the missMDA (Josse and Husson, 2016) and SVA (Leek *et al.*, 2012) R packages, respectively. For the vast majority of body sites (33/48), SVA identified zero significant surrogate variables. Nevertheless, as an extra precaution against confounders, we ran all regression analyses including one surrogate variable.

Partitioning samples per body site and histological type, we identified sites that significantly associated with age ($|beta_{age}| > 0.01$ and FDR < 0.1) through REDIT-Regression using the surrogate variables and age as covariates. Tissues with an increasing trajectory in editing over age were defined as those where the number of editing sites demonstrating an increasing trend is at least twice of that with a decreasing trend (and Fisher's exact test FDR < 0.1). Tissues with a decreasing trajectory were defined similarly. The same criteria were used when finding editing sites associated with age in a dataset of 33 postmortem frontal cortex samples (Hwang *et al.*, 2016). The subset of samples used to match the age range of GTEx frontal cortex samples were R4054 age: 40.6, R2897 age: 41.0, R4049 age: 41.2, R4371 age: 41.8, R3791 age: 42.1, R2826 age: 42.8, R3539 age: 57.5, R3479 age: 58.6, R3766 age: 59.3, R3445 age: 61.2, R4038 age: 67.9 and R3990 age: 71.1.

To identify editing sites that significantly associate with gender, we ran REDIT-Regression using gender, the surrogate variables and age as covariates, since age is already a known variable correlated with editing (Dillman *et al.*, 2013; Hwang *et al.*, 2016; Li *et al.*, 2013; Wahlstedt *et al.*, 2009). $|Beta_{sex}| > 0.05$ and FDR < 0.1 were used to call significant associations.

### 2.10 Application of REDIT-LLR to identify distinct recoding profiles across brain regions

To find differential recoding sites between pairs of brain regions, we used REDIT-LLR to test editing sites annotated as non-synonymous in REDIPortal (4388 non-synonymous editing sites). Recoding sites with differences in average editing levels >0.05 and FDR <0.1 were considered differential.

### 2.11 Implementing statistical tests

The *t*-test, Wilcoxon rank-sum test, Fisher's exact test and linear regression were performed using corresponding base functions in R. Binomial regression was run in R using the gamlss package (version 5.1-2) using default arguments. LIMMA was run using the LIMMA package (version 3.42.0) with parameters to incorporate a mean-variance trend and variance robustified against outlier sample variance.

### 2.12 Running-time performance evaluation

The running-time performances of the REDIT-LLR and REDIT-Regression were evaluated by running various numbers of editing sites from real datasets. REDIT-LLR was run on 29 Autism and 33 controls from frontal cortex (Tran *et al.*, 2019), and REDIT-Regression was run on the 33 frontal cortex samples spanning human development (Hwang *et al.*, 2016). We calculated the average running-time (average time required to run one editing site) by fitting a least-squares linear regression on running-time (min) versus number of editing sites tested. No computational parallelization was used for these evaluations.

## 3 Results

### 3.1 Overview of REDITs

REDITs model read counts in RNA editing using a beta-binomial distribution, where read coverage is modeled using the binomial component, and biological variance between replicates is concurrently modeled with the beta component. For differential editing tests between groups (e.g. cases versus controls), REDITs evaluate a null model assuming no between-group difference, compared to an alternative model that includes two distinct groups. It then determines differential editing based on the significance of the likelihood ratio of the two models (thus, called REDIT-LLR, Fig. 1a and b). To test the correlation of an editing site with one or multiple biological factors (e.g. covariance of editing with age), REDITs model the covariates as a linear combination of regressors that together constitute the mean of the beta component. It then tests whether inclusion of each covariate significantly improves the maximum likelihood ratio (thus, called REDIT-Regression, Fig. 1a and c).

### 3.2 Evaluation of the REDIT-LLR method via simulated data

To evaluate the REDIT-LLR method, we simulated read counts of editing sites using beta distributions estimated from GTEx brain

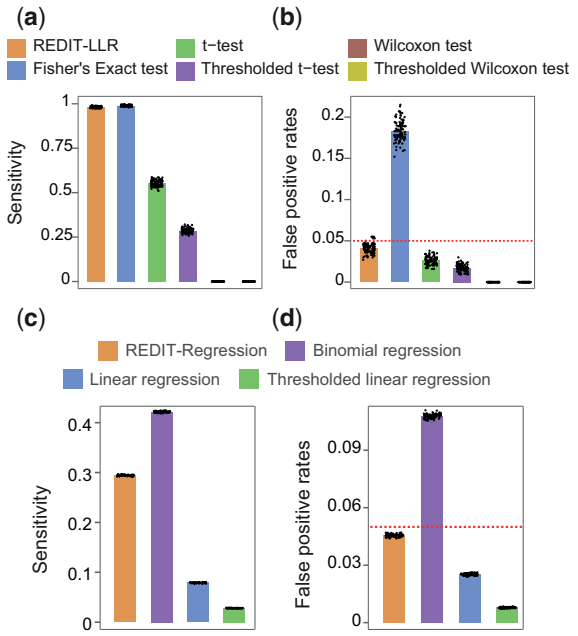


**Fig. 2.** Evaluation of REDITs using simulated data. (**a**) Sensitivity of REDIT-LLR was evaluated using simulations where group 1 editing level was characterized by beta($\alpha$=13.52, $\beta$=11.95) and group 2 as beta($\alpha$=43.64, $\beta$=0.23) with three samples per group. (**b**) False-positive rate was evaluated where both group1 and group2 were simulated as beta($\alpha$=13.52, $\beta$=11.95). (**c**) Sensitivity of REDIT-Regression was evaluated where editing level was characterized as a beta distribution with mean simulated as $\mu_i$=0.005*$A_i$ +0.33 over three samples. (**d**) False-positive rate was evaluated where age had no simulated effect on editing levels. Individual points show 100 replicate simulation results. Red dotted lines show the 5% false-positive rate threshold. Thresholded *t*-test and thresholded Wilcoxon test =*t*-test and Wilcoxon rank-sum test run on samples with minimal 10 read coverage. Thresholded linear regression = linear regression on only samples with minimal 10 read coverage. REDITs have highest sensitivities out of all tests that remain within a 5% false-positive rate

tissues (Supplementary Fig. S1a–c and Table S1b and c). We simulated 2, 3 or 5 biological replicates per group, which are typical sample sizes in case–control studies. The significance level was chosen to be 0.05. REDIT-LLR had much greater sensitivity (true-positive rate) than the *t*-test or Wilcoxon rank-sum test, particularly for smaller sample sizes (Fig. 2a and Supplementary Fig. S2), which is consistent with the lack of depreciation of sites with inadequate coverages by the latter two methods. Also, this problem of the two methods is not alleviated using thresholds to impose a minimal coverage requirement (Fig. 2a and Supplementary Fig. S2), due to loss of sample size.

Although the Fisher's exact test has comparable sensitivity as REDIT-LLR, its false-positive rate is much higher than the nominal level of 0.05 and that of REDIT-LLR (Fig. 2b and Supplementary Fig. S2). This limitation of Fisher's exact test is consistent with its theoretical flaw of neglecting biological variability. Notably, this problem of Fisher's exact test exacerbates as sequencing coverage increases (Supplementary Fig. S3).

As an alternative method, we simulated editing sites using a different hyper-parameter distribution (truncated normal instead of beta distribution) (Supplementary Fig. S1d). The REDIT-LLR method still outperformed the other methods (Supplementary Fig. S4), indicating that this method is robust to the underlying distribution of editing levels.

### 3.3 Evaluation of the REDIT-LLR method using actual RNA-seq data

We evaluated the false-positive rates of different methods by randomly grouping control samples of a previous study (Hung *et al.*, 2015) into two groups (Section 2). Editing sites identified with $P < 0.05$ were considered as false-positive predictions. REDIT-LLR yielded the lowest false-positive rates in the majority of comparisons and across all sample sizes (Supplementary Fig. S5a). All methods except Fisher's exact test had false-positive rates <5%. In particular, Fisher's exact test performed poorly at editing sites with highly variable editing levels between samples, which are enriched in Alu and intronic regions (Supplementary Fig. S5b and c). In contrast, for sites with lower variability, which were enriched in exonic and non-Alu regions, Fisher's exact test performed adequately (false-positive rates < 5%). The assumption of low variance between biological replicates likely holds for these editing sites where precise regulation of editing level may be critical for homeostasis (Pinto *et al.*, 2014).

To evaluate the sensitivity of each method, we leveraged a previous dataset containing two replicates of ADAR1 KD and controls in U87 cells (Bahn *et al.*, 2012). As reduced ADAR1 expression is expected to result in editing reduction, we used the number of differential editing sites called by each method as a proxy for sensitivity. REDIT-LLR had higher sensitivity than all the other methods except Fisher's exact test (which suffers from high false-positive rates) (Supplementary Fig. S6a). In particular, REDIT-LLR was able to identify differential editing sites with relatively low baseline levels or small effect sizes (Supplementary Fig. S6b).

### 3.4 Evaluation of the REDIT-Regression method

To evaluate the REDIT-Regression method, we simulated editing sites based on RNA-seq data of 33 postmortem frontal cortex samples used in a study of RNA editing in human development (Hwang *et al.*, 2016). The simulations incorporated unaltered read coverages per editing site from the actual data. To evaluate sensitivity, we simulated editing sites that covary with age ($\beta_{age}$and $\beta_0$ parameters) (Supplementary Table S1d and Fig. S7a and b). For all simulations and across various tested sample sizes, the REDIT-Regression method had higher sensitivity (proportion of sites with $P < 0.05$) than the linear regressions, though lower sensitivity than binomial regression (Fig. 2c and Supplementary Fig. S8a). Similar trends were observed using simulated data generated from a truncated normal instead of beta distribution (Supplementary Fig. S9a).

We also used the same 33 samples as described above, but did not impose any correlation between RNA editing and age. Thus, the prediction of a significant association between editing and age is a false positive. Based on these simulations across multiple sample sizes, the false-positive rate of REDIT-Regression remains at or below 5%, whereas binomial regression and LIMMA yielded much

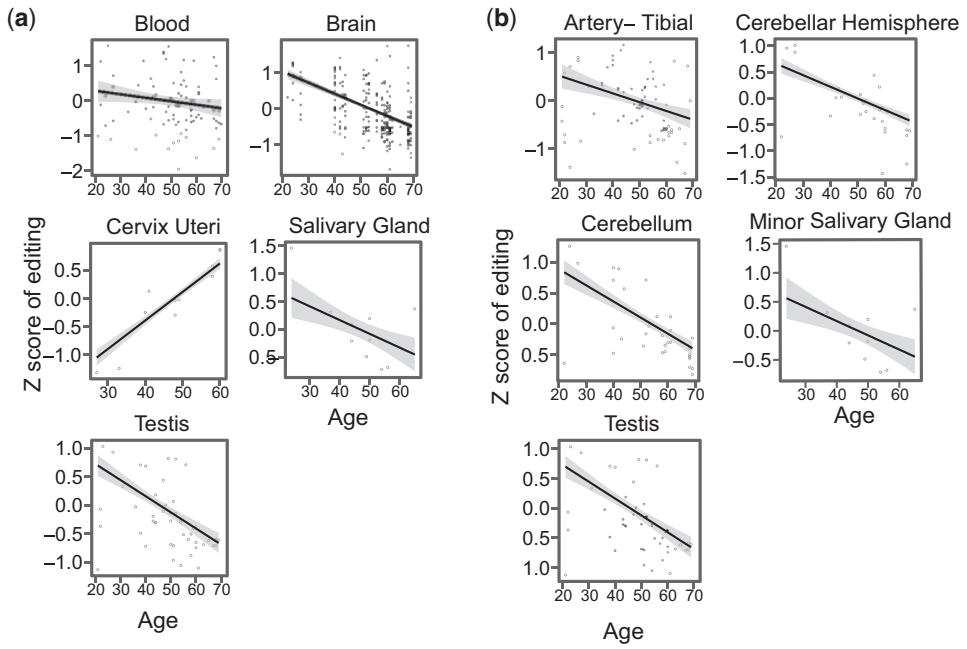


**Fig. 3.** REDIT-Regression uncovers overall trends of RNA editing over human aging. REDIT-Regression was performed to find RNA-editing levels that statistically associate with age. Plots show linear regression lines fit to *z*-scores of all RNA-editing sites that were found significantly associated with age in samples partitioned by tissue type. Only tissue types exhibiting homogenous trajectories of editing over age are plotted (Supplementary Table S2a). (**a**) Tissues partitioned by histological type. (**b**) Tissues partitioned by body site. Gray shading shows the 99% confidence interval from regression. Points show the median *z*-score per sample

higher false-positive rates (Fig. 2d and Supplementary Figs S8b, S9b and S10a and b). Strikingly, LIMMA had inordinately inflated false-positive rates, prompting us to exclude it from any further comparison (Supplementary Fig. S10a and b).

We next evaluated the false-positive rate of REDIT-Regression using actual RNA-seq data by bootstrapping samples and shuffling the associated random covariate values (Section 2). Similar to the simulation results, all methods except the binomial regression maintained false-positive rates below 5% across all sample sizes (Supplementary Fig. S11).

Overall, out of the methods that mitigate false positives to 5%, REDIT-Regression had the highest sensitivity, demonstrating the optimal balance between false- and true-positive rate.

### 3.5 REDIT-Regression on GTEx data uncovers association of RNA editing with human aging

Multiple studies indicate that RNA-editing levels in the brain increase over age (Dillman *et al.*, 2013; Hwang *et al.*, 2016; Li *et al.*, 2013; Wahlstedt *et al.*, 2009). However, this trend has not been evaluated across many samples for the panoply of human tissues. We applied REDIT-Regression to the GTEx dataset, to comprehensively investigate the trajectory of editing variations over human aging. Overall, most tissues had few age-associated editing sites (Supplementary Table S2a and b). However, there were a few exceptions, such as brain, testis and cervix, which had hundreds of age-associated sites. Interestingly, many of these tissues also exhibited homogenously increasing or decreasing trajectories of editing (Supplementary Table S2a and b and Fig. 3a and b).

One striking observation in our results is that editing decreased with age in the brain (Fig. 3a and b). A previous study reported an increasing trend of brain editing with age (frontal cortex) (Hwang *et al.*, 2016). However, this increasing trend was predominantly driven by the fetal to infant transition, which was replicated in another study (Tran *et al.*, 2019). The ages of GTEx subjects ranged from 20 to 70 years (Supplementary Fig. S12a and b), which only encapsulate the period of human adulthood to older age. Thus, we hypothesized that the disparity in the age-editing association between ours and previous studies (Dillman *et al.*, 2013; Hwang *et al.*, 2016; Li *et al.*, 2013; Wahlstedt *et al.*, 2009) was attributable to differences in the ages of the respective cohorts. To level the comparison, we performed REDIT-Regression in two ways using the previous dataset (Hwang *et al.*, 2016), with the entire cohort and with a subset of frontal cortex samples aged $\geq$ 20 years, respectively. REDIT-Regression on the entire cohort recapitulated that editing levels predominantly increased during development (762 sites increasing versus 148 sites decreasing, $\chi^2$ $P$-value $= 3.1e^{-54}$, odds ratio $=5.14$). However, in the subset of samples aged $\geq$ 20 years, REDIT-Regression identified no editing sites associated with age, which is similar to that observed in the GTEx samples where only seven sites were associated with age (brain-frontal cortex, Supplementary Table S2b). Overall, our findings underscore that the trends of RNA-editing changes differ between early development versus aging.

### 3.6 REDIT-Regression on GTEx data reveals gender-biased RNA editing

Although humans display sexual dimorphism in morphology and physiology, RNA-editing differences between genders is largely unknown. Recent studies implicated RNA editing in gender-specific stratification of glioblastoma survival (Silvestris *et al.*, 2019). However, comprehensive investigation of gender-biased editing across human tissues has not been reported. We carried out REDIT-Regression analysis on the GTEx dataset using both age, a surrogate variable (Section 2), and gender as covariates. Strikingly, we observed hundreds of gender-biased editing sites across diverse tissue types (Fig. 4 and Supplementary Fig. S13) (FDR $< 0.1$ in Section 2). Tissues with the greatest number of gender-associated sites, included the tibial nerve, thyroid, pancreas, skin and adipose, some of which also exhibit physiological differences between genders (Fuente-Martin *et al.*, 2013; Gannon *et al.*, 2018; Giacomoni *et al.*, 2009).

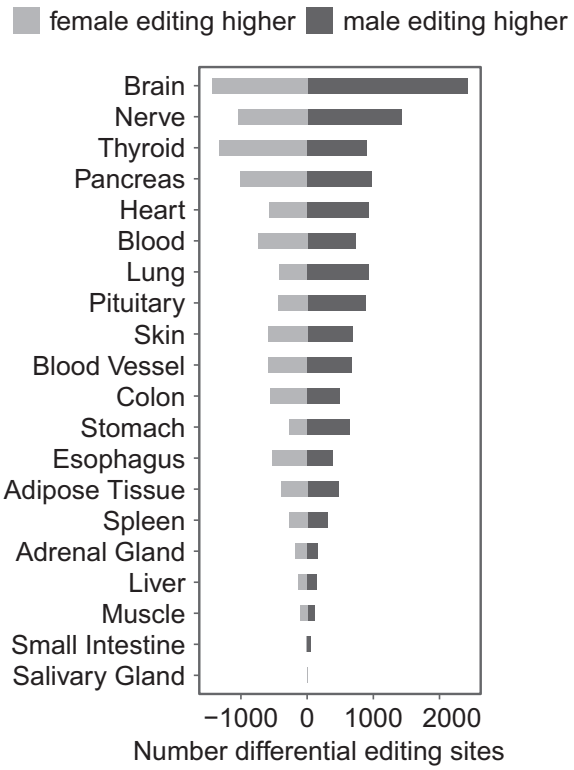


**Fig. 4.** Gender-biased RNA editing in various tissues. REDIT-Regression was performed across GTEx tissues partitioned by histological type to find editing sites associated with gender. Bargraphs show number of editing sites found significantly more highly edited in males (dark grey) or females (light grey). Significant sites defined with FDR <0.1 and mean difference between genders >0.05

Our observation suggests that gender-specific RNA editing may be involved in sexual dimorphism of different aspects of physiology.

### 3.7 REDIT-LLR unveils distinct protein-recoding profiles between brain regions

Next, we applied REDIT-LLR to test whether the various brain regions in human have distinct protein-recoding profiles. Many brain regions displayed dozens of differential recoding events (Supplementary Fig. S14 and Table S3). For example, the glutamine to arginine recoding event in GRIA2 (Behm and Öhman, 2016) (edited at ~100% in cerebellum) has ~10% lower editing in amygdala, hypothalamus, putamen, caudate, hippocampus, and ~20% lower editing in the substantia nigra (Supplementary Table S3). Strikingly, the cerebellar regions had particularly disparate recoding profiles relative to all other brain regions (Supplementary Fig. S14), consistent with its substantial differences in cellular composition and neurophysiology (Rakic, 2009). Overall, these observations suggest that RNA recoding events may be associated with regional differences of the human brain.

### 3.8 Computational speed of REDITs

We evaluated REDITs run-time using data from two previous studies (62 samples in the LLR analysis, and 33 samples in the regression analysis) (Hwang *et al.*, 2016; Tran *et al.*, 2019). The REDIT-LLR method processed 100 000 editing sites in about 14 min (Fig. 5a). REDIT-Regression ran 36 min for 100 000 editing sites (Fig. 5b). For the preponderance of RNA editing studies, this level of speed is efficient and should obviate the need for parallelization, permitting application of the methods given the most basic computational

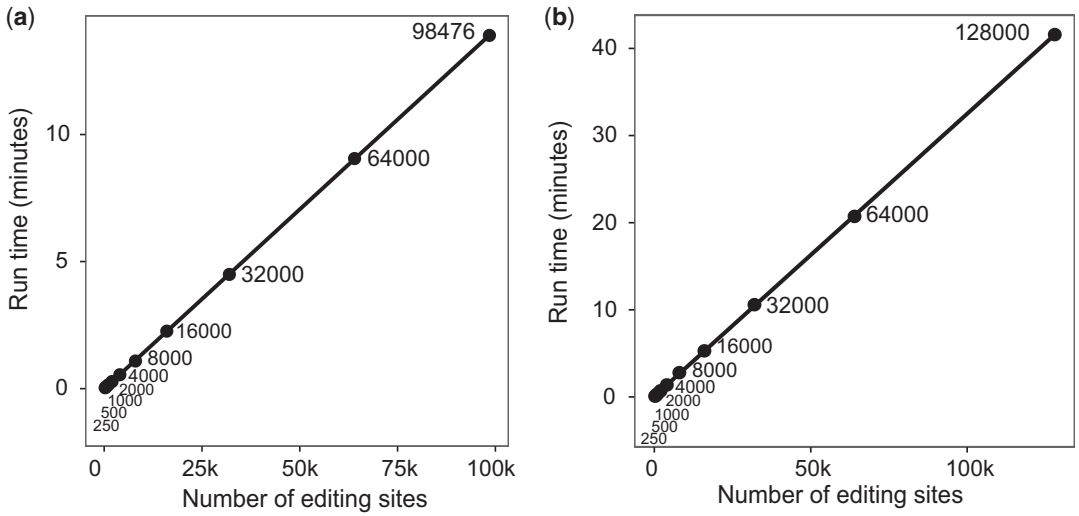


**Fig. 5.** Computational speed of REDITs. The points in the scatterplots show the run time (min) in analyzing various numbers of editing sites from real datasets. (**a**) Computational run time of REDIT-LLR. (**b**) Computational run time of REDIT-Regression. Annotations specify the exact numbers of editing sites tested. The fitted lines were derived by least-squares regression

resources. Nevertheless, we provide an example of how to include parallelization in the REDITs codes (see code availability).

## 4 Discussion

In this work, we introduce REDITs which leverage beta-binomial models to detect editing differences between groups or editing association with covariates. Compared to nominal methods used in previous studies, REDITs proffer the advantage of handling the uncertainty in RNA-editing levels calculated from limited sequencing depth in RNA-seq data, while still maintaining biological variance modeling. Using both simulated and actual data, we demonstrated that REDITs have superior performance than commonly utilized tests in RNA-editing studies. Consistently across simulations, REDITs proffered the highest gains in sensitivity in relatively small sample sizes, particularly advantageous for cases with high costs of sample attainment and RNA-seq. Since REDITs consider biological replicates to model the variability across data sets, they are particularly suitable for handling data with sparse and limited counts. If the sequencing depth is very high, REDITs mathematically simplify to a likelihood ratio test of beta distributions for case–control studies, or a beta regression for regression analyses. Since most RNA-seq data have limited coverage at the single-nucleotide level, REDITs serve a widespread utility. Additionally, the underlying beta-binomial model can be applied to other questions, such as detecting allelic expression biases and expression of somatic mutations in cancer.

In this study, we clarified the trajectory of editing changes associated with age in human tissues. Although most tissues had few editing sites associated with age, some exceptions were present, including brain, testis and cervix, which had hundreds of age-associated sites. Many of these tissues also exhibited homogenously

increasing or decreasing trajectories of editing over age. Our analyses also clarified that, in brain, editing level increases during early development, and then decreases from adulthood to old age. Interestingly, most tissues also had hundreds of RNA-editing sites with gender bias, which may contribute to sexual differences in physiology and anatomy. Lastly, multiple brain regions, particularly cerebellum, had distinct editing levels of protein-recoding sites, including those with neuronal salience, which could contribute to regional differences. The functional importance and mechanistic underpinnings of these trends merit additional validation and further examination. Overall, REDITs should serve prodigiously to expand our understanding of how RNA editing undergirds molecular systems, biological phenotypes and disease.

## Sample availability

The data from GTEx are available on the GTEx portal (https://gtexportal.org/home/). Data from REDIportal are downloadable from http://srv00.recas.ba.infn.it/atlas/index.html. Autism and control samples are available in the PsychENCODE website (https://www.synapse.org//#! Synapse: syn4587609). The data from 33 postmortem brains from Hwang *et al.* are available on NCBI SRA (SRP076099). Data from the cohort with Systemic Lupus Erythematosus are available on GEO, accession number GSE72420. RNA-sequencing from ADAR1 knock-down and control U87 cell lines is available on GEO, accession number GSE28040.

## Acknowledgements

We thank the GTEx Project for generating the valuable datasets used in this study. We would also like to thank the members of the Xiao laboratory for their helpful discussions and comments on this work.

## Funding

This work was supported in part by grants from the National Institute of Health [U01HG009417, U01CA204695].

*Conflict of Interest*: none declared.

## References

Bahn,J.H. *et al.* (2012) Accurate identification of A-to-I RNA editing in human by transcriptome sequencing. *Genome Res.*, **22**, 142–150.

Bahn,J.H. *et al.* (2015) Genomic analysis of ADAR1 binding and its involvement in multiple RNA processing pathways. *Nat. Commun.*, **6**, 6355.

Behm,M. and Öhman,M. (2016) RNA editing: a contributor to neuronal dynamics in the mammalian brain. *Trends Genet.*, **32**, 165–175.

Brummer,A. *et al.* (2017) Structure-mediated modulation of mRNA abundance by A-to-I editing. *Nat. Commun.*, **8**, 1255.

Chen,L. *et al.* (2013) Recoding RNA editing of AZIN1 predisposes to hepatocellular carcinoma. *Nat. Med.*, **19**, 209–216.

Dillman,A.A. *et al.* (2013) mRNA expression, splicing and editing in the embryonic and adult mouse cerebral cortex. *Nat. Neurosci.*, **16**, 499–506.
Dolzhenko,E. and Smith,A.D. (2014) Using beta-binomial regression for high-precision differential methylation analysis in multifactor whole-genome bisulfite sequencing experiments. *BMC Bioinformatics*, **15**, 215.
Feng,Y. *et al.* (2006) Altered RNA editing in mice lacking ADAR2 autoregulation. *Mol. Cell. Biol.*, **26**, 480–488.
Feng,H. *et al.* (2014) A Bayesian hierarchical model to detect differentially methylated loci from single nucleotide resolution sequencing data. *Nucleic Acids Res.*, **42**, e69.
Fuente-Martin,E. *et al.* (2013) Sex differences in adipose tissue: it is not only a question of quantity and distribution. *Adipocyte*, **2**, 128–134.
Fumagalli,D. *et al.* (2015) Principles governing A-to-I RNA editing in the breast cancer transcriptome. *Cell Rep.*, **13**, 277–289.
Gannon,M. *et al.* (2018) Sex differences underlying pancreatic islet biology and its dysfunction. *Mol. Metab.*, **15**, 82–91.
Giacomoni,P.U. *et al.* (2009) Gender-linked differences in human skin. *J. Dermatol. Sci.*, **55**, 144–149.
Han,L. *et al.* (2015) The genomic landscape and clinical relevance of A-to-I RNA editing in human cancers. *Cancer Cell*, **28**, 515–528.
Hebestreit,K. *et al.* (2013) Detection of significantly differentially methylated regions in targeted bisulfite sequencing data. *Bioinformatics*, **29**, 1647–1653.
Hideyama,T. *et al.* (2012) Profound downregulation of the RNA editing enzyme ADAR2 in ALS spinal motor neurons. *Neurobiol. Dis.*, **45**, 1121–1128.
Hsiao,Y.E. *et al.* (2018) RNA editing in nascent RNA affects pre-mRNA splicing. *Genome Res.*, **28**, 812–823.
Hung,T. *et al.* (2015) The Ro60 autoantigen binds endogenous retroelements and regulates inflammatory gene expression. *Science*, **350**, 455–459.
Hwang,T. *et al.* (2016) Dynamic regulation of RNA editing in human brain development and disease. *Nat. Neurosci.*, **19**, 1093–1099.
Ishizuka,J.J. *et al.* (2019) Loss of ADAR1 in tumours overcomes resistance to immune checkpoint blockade. *Nature*, **565**, 43–48.
Josse,J. and Husson,F. (2016) missMDA: a package for handling missing values in multivariate data analysis. *J. Stat. Softw.*, **70**, 31.
Kang,L. *et al.* (2015) Genome-wide identification of RNA editing in hepatocellular carcinoma. *Genomics*, **105**, 76–82.
Leek,J.T. *et al.* (2012) The sva package for removing batch effects and other unwanted variation in high-throughput experiments. *Bioinformatics*, **28**, 882–883.
Li,Z. *et al.* (2013) Evolutionary and ontogenetic changes in RNA editing in human, chimpanzee, and macaque brains. *RNA*, **19**, 1693–1702.
Liddicoat,B.J. *et al.* (2015) RNA editing by ADAR1 prevents MDA5 sensing of endogenous dsRNA as nonself. *Science*, **349**, 1115–1120.
Nishikura,K. (2016) A-to-I editing of coding and non-coding RNAs by ADARs. *Nat. Rev. Mol. Cell Biol.*, **17**, 83–96.
Park,Y. *et al.* (2014) MethylSig: a whole genome DNA methylation analysis pipeline. *Bioinformatics*, **30**, 2414–2422.
Paz,N. *et al.* (2007) Altered adenosine-to-inosine RNA editing in human cancer. *Genome Res.*, **17**, 1586–1595.
Paz-Yaacov,N. *et al.* (2015) Elevated RNA editing activity is a major contributor to transcriptomic diversity in tumors. *Cell Rep.*, **13**, 267–276.
Picardi,E. *et al.* (2017) REDIportal: a comprehensive database of A-to-I RNA editing events in humans. *Nucleic Acids Res.*, **45**, D750–D757.
Picardi,E. *et al.* (2015) Profiling RNA editing in human tissues: towards the inosinome Atlas. *Sci. Rep.*, **5**, 14941.
Pinto,Y. *et al.* (2014) Mammalian conserved ADAR targets comprise only a small fragment of the human editosome. *Genome Biol.*, **15**, R5.
Qin,Y.R. *et al.* (2014) Adenosine-to-inosine RNA editing mediated by ADARs in esophageal squamous cell carcinoma. *Cancer Res.*, **74**, 840–851.
Quinones-Valdez,G. *et al.* (2019) Regulation of RNA editing by RNA-binding proteins in human cells. *Commun. Biol.*, **2**, 19.
Rakic,P. (2009) Evolution of the neocortex: a perspective from developmental biology. *Nat. Rev. Neurosci.*, **10**, 724–735.
Roth,S.H. *et al.* (2018) Increased RNA editing may provide a source for autoantigens in systemic lupus erythematosus. *Cell Rep.*, **23**, 50–57.
Rueter,S.M. *et al.* (1999) Regulation of alternative splicing by RNA editing. *Nature*, **399**, 75–80.
Silvestris,D.A. *et al.* (2019) Dynamic inosinome profiles reveal novel patient stratification and gender-specific differences in glioblastoma. *Genome Biol.*, **20**, 33.
Srivastava,P.K. *et al.* (2017) Genome-wide analysis of differential RNA editing in epilepsy. *Genome Res.*, **27**, 440–450.
Stellos,K. *et al.* (2016) Adenosine-to-inosine RNA editing controls cathepsin S expression in atherosclerosis by enabling HuR-mediated post-transcriptional regulation. *Nat. Med.*, **22**, 1140–1150.
Sun,D. *et al.* (2014) MOABS: model based analysis of bisulfite sequencing data. *Genome Biol.*, **15**, R38.
Tan,M.H. *et al.*; GTEx Consortium. (2017) Dynamic landscape and regulation of RNA editing in mammals. *Nature*, **550**, 249–254.
Tran,S.S. *et al.* (2019) Widespread RNA editing dysregulation in brains from autistic individuals. *Nat. Neurosci.*, **22**, 25–36.
Wahlstedt,H. *et al.* (2009) Large-scale mRNA sequencing determines global regulation of RNA editing during brain development. *Genome Res.*, **19**, 978–986.
Yablonovitch,A.L. *et al.* (2017) The evolution and adaptation of A-to-I RNA editing. *PLoS Genet.*, **13**, e1007064.